Bulletin of the *Transilvania* University of Braşov
Series I: Engineering Sciences • Vol. 6 (55) No. 2 - 2013

SMALL WIND TURBINE CONTROL WITH FREQUENCY SUPPORT FOR INTEGRATION IN MICROGRIDS

Ioan ŞERBAN[1]

Abstract: *Enhancing the controllability of small wind turbines (WT) to support the frequency in microgrids (MG) requires different solutions than for high power WT. This paper presents a sensorless control method for small fixed-pitch WT, which includes, besides the primarily function of WT optimal control, a power curtailment technique that aims to improve the MG stability during adverse operating conditions. Simulation results are presented to validate the proposed method.*

Key words: *small wind turbine, microgrid, frequency control, single-phase inverter.*

1. Introduction

One concept of the future smart grid considers the microgrid (MG) as the main building block, where they can operate autonomously or interconnected in clusters [4]. Aiming towards a sustainable and clean way to supply electricity in the future, the renewable energy sources (RES) will have a major contribution in powering the MG. Nevertheless, the inherent RES power intermittency and the difficult predictability affect the system reliability and security, while the stability, like the frequency stability, may be seriously jeopardized once the RES penetration level becomes too high [1].

Frequency control represents a main component within the control system of an MG, being the process involving the management of the energy resources within the system. Among various control methods that can be adopted to ensure the frequency stability of an MG [3], [7], [8] (e.g. using energy storage and smart loads), this paper focuses on the controllability of the RES generators in order to support the MG. The major challenge consist in the fact that RES generators output power strongly depends on exogenous factors, as weather conditions, thus lacking the controllability of classical generators. This paper proposes a method to enhance the small wind turbines (WT) integrated in autonomous MGs with frequency support. Several studies address the tackled issue [2], [9], [15], while the majority focuses on high power wind turbines connected to the grid. Small WT (kW-range) have much less control possibilities on the mechanical side (e.g. without pitch mechanism) and therefore being more difficult to control their output power when demanded [6].

To be mentioned that this paper continues the work from [9], where the

[1] Dept. of Electrical Engineering, *Transilvania* University of Braşov.

optimal control of the WT by means of a sensorless method was presented and therefore this paper will only focuses on the new aforementioned contribution.

After the introduction, the paper is organized as follows: section 2 describes the WT components, the proposed control method is validated and discussed in section 3, while the paper main conclusions are highlighted in section 4.

2. System Description

The small WT configuration is shown in Figure 1, where it contains a kW-range, three-blade, fixed-pitch wind rotor, gearless connected to a multi-pole three-phase permanent magnet synchronous generator (PMSG), a diode rectifier bridge, followed by the DC side. The rectified voltage filtered by a DC capacitor is then applied to a boost converter, which supplies the DC-link of a single-phase inverter to the required voltage level. The H-bridge inverter along with a low-pass filter accomplishes the interface between the WT DC-side and the MG. A DC dump load is added to consume the excess power produced by the WT in certain conditions, protecting both the generator against overspending and the DC-link against over voltage.

Controlling the output power of a fixed blade WT connected to an MG to support the MG frequency represents an important feature [12]. In this paper, a sensorless control method is proposed to control the WT output power and rotor speed, while also supporting the MG frequency under adverse operating conditions.

2.1. WT-Generator-Rectifier

The subsystem including the wind rotor, generator and rectifier is detailed in [9]. The mechanical torque produced by the wind rotor for a fixed-pitch, horizontal-axis wind turbine can be expressed by the following equation [11]:

$$\Gamma_{WT}(\omega_r, v_w) = 0.5\,\pi R^2 \rho C_p(\lambda) v_w^3 \cdot \omega_r^{-1}, \quad (1)$$

where: ω_r is the rotor angular velocity, ρ is the air mass density, R is the blade radius, v_w is the wind speed; $C_p(\lambda)$ is the power coefficient of the wind turbine and λ is the tip-speed ratio of the rotor blade tip speed to wind speed.

The wind turbine rotor interacts with the generator by means of a rigid shaft, and therefore a one-mass equivalent model of the mechanical drive train is adopted, represented by the following expression:

$$J \frac{d\omega_r}{dt} = \Gamma_{WT} - \Gamma_{PMSG}, \quad (2)$$

where: J is the combined moment of inertia of generator and turbine, while Γ_{PMSG} represents the mechanical load torque produced by the generator.

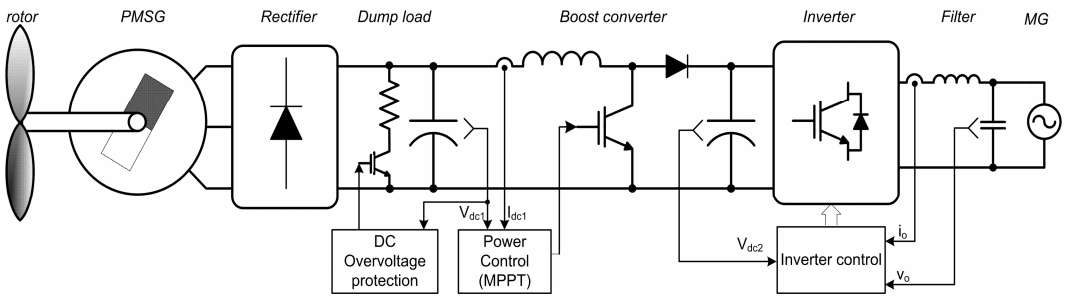

Fig. 1. *The WT configuration*

The generator mechanical torque can be expressed as follows:

$$\Gamma_{PMSG} = \frac{P_{dc} + \Delta P}{\omega_r}, \quad (3)$$

where: P_{dc} is the rectifier output power; ΔP is the sum of the losses on the generator and rectifier.

The rectifier output DC voltage (V_{dc1}) depends on several operating parameters of the generator-rectifier-load system, as detailed in [14]. However, for continuous conduction mode, when the output current is continuous, the DC voltage can be approximated by the following expression:

$$V_{dc1} = \frac{3\sqrt{3}}{\pi} V_m - \left(\frac{3}{\pi} \omega_e L_S + 2R_S \right) I_{dc1}, \quad (4)$$

where: L_S, R_S are the resistance and inductance of the stator (neglecting the cables and rectifier resistances); V_m is the magnitude of the PMSG internal line-to-neutral voltage; $\omega_e = \omega_r / P$ is the electrical pulsation, with P being the number of pole pairs of the generator.

2.2. Boost Converter

The main purpose of the boost converter is to raise the DC voltage, which comes from the rectifier, at the required level for the inverter input, i.e. between 350-400 V. It also accomplishes maximum power point tracking (MPPT), in order to maximize electrical power produced by the wind generator. Figure 2 illustrates the scheme of the boost converter, whereas the control block diagram is detailed in Figure 3. The rectified DC voltage value (V_{dc1}) is provided to a look-up table that implements a predefined maximum power point (MPP) characteristic (shown in Figure 4a), which further generates the DC current reference (I_{dc1}^*). A PI controller amplifies the error between the reference and measured currents providing the duty-cycle of the PWM signal that drives the transistor within the boost converter.

As mentioned before, the proposed system is designed to support the MG frequency, namely the WT can decrease its output power when the MG frequency exceeds a certain threshold. This feature is implemented in the boost converter control (Figure 3b), by applying a curtailment factor (k_{md}) on the MPP characteristic. The goal is to deflect the operating point from the optimal value, thus reducing the WT output power. Figure 4b shows the MPP curtailment characteristic function of the MG frequency. As the MG frequency increases above 50.5 Hz, the WT output power is gradually reduced down to zero at 51 Hz.

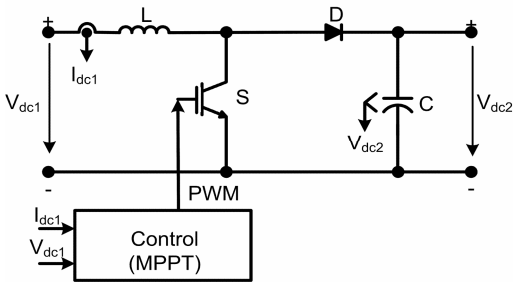

Fig. 2. *Boost converter*

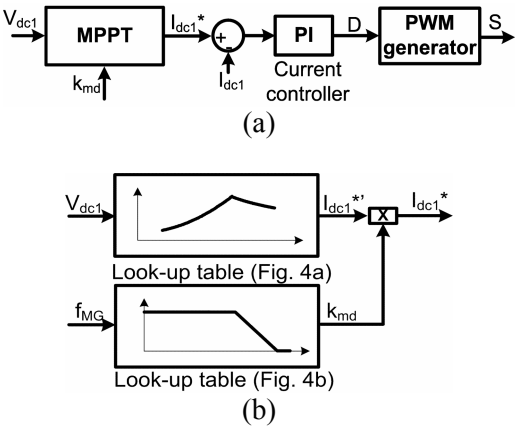

Fig. 3. *Boost converter control: a) overall control block diagram; b) current reference generation (I_{dc1}^*)*

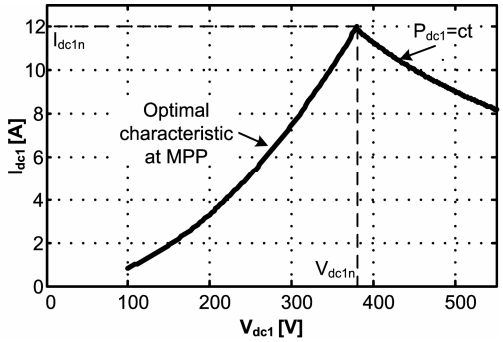

(a)

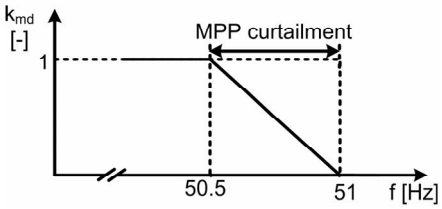

(b)

Fig. 4. *WT control characteristics: a) $I_{dc1} = f(V_{dc1})$ characteristic; b) MPP curtailment coefficient (k_{md}) depending of the MG frequency*

2.3. Single-Phase Inverter

The inverter is controlled to inject active power and no reactive power to the MG, operating as a grid-feeding inverter. The control block diagram, shown in Figure 5, is based on two PI current controllers applied in a fictitious synchronous reference frame (SRF) created by means of a frequency-adaptive quadrature signal generator (QSG) [13]. The AC side voltage (v_o) is transformed in two quadrature voltages $v_{o\alpha}$ and $v_{o\beta}$, corresponding to the α-β stationary reference frame. The two voltage components are transformed in the synchronous reference frame (dq) by means of a αβ-dq transformation block, providing the unfiltered voltage components V_{od} and V_{oq} after the following equations:

$$V_{od} = v_{o\alpha}\cos(\theta) + v_{o\beta}\sin(\theta), \tag{5}$$

$$V_{oq} = -v_{o\alpha}\sin(\theta) + v_{o\beta}\cos(\theta). \tag{6}$$

The inverter output current (i_o) undergoes the same transformations, as follows:

$$I_{od} = i_{o\alpha}\cos(\theta) + i_{o\beta}\sin(\theta), \tag{7}$$

$$I_{oq} = -i_{o\alpha}\sin(\theta) + i_{o\beta}\cos(\theta). \tag{8}$$

Because the MG voltage may be affected by harmonics, two Butterworth low-pass filters (LPF) are used as shown in Figure 5, resulting the voltages V_{odf} *and* V_{oqf}.

A standard single-phase phase-locked loop (PLL) is used to synchronize the inverter with the MG voltage and to provide

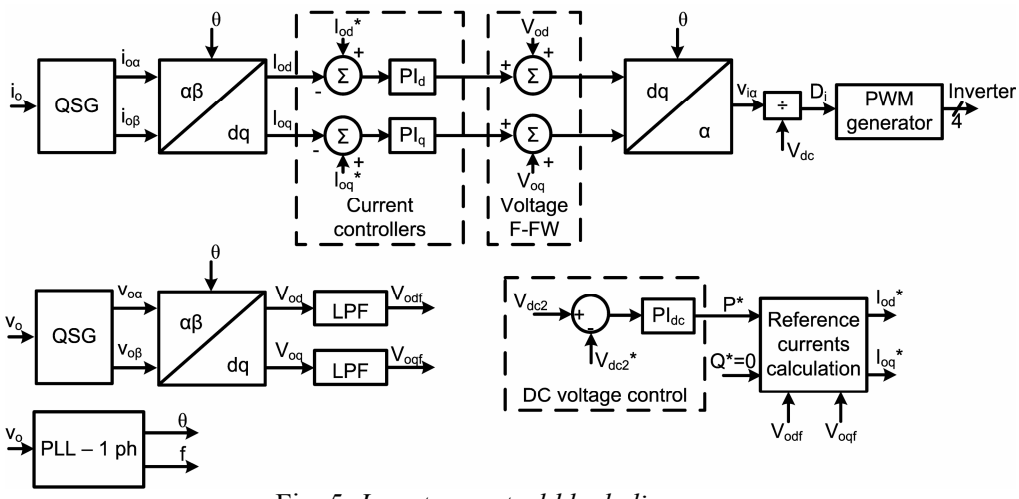

Fig. 5. *Inverter control block diagram*

the reference phase θ required by the SRF transformations [5]. As additional signal, the PLL also provides also the MG frequency, which is used by the MPP curtailment control block.

A DC-voltage controller (PI_{dc}) gives the active power reference (P^*), while the reactive power reference is set to zero (no voltage support is implemented in this case). The reference currents I_{od}^* and I_{oq}^* in d-q reference frame are generated using the reference active and reactive powers P^*, Q^* and the two filtered voltage components V_{odf}, V_{oqf} in d-q reference frame, as follows:

$$I_{od}^* = \frac{2(P^* V_{odf} - Q^* V_{oqf})}{V_{odf}^2 + V_{oqf}^2}, \quad (9)$$

$$I_{oq}^* = \frac{2(P^* V_{oqf} + Q^* V_{odf})}{V_{odf}^2 + V_{oqf}^2}. \quad (10)$$

The output voltages resulting from the two current controllers (PI_d, PI_q) are added with the unfiltered voltage components V_{od} and V_{oq}, in d-q reference frame (this is a voltage feed-forward to improve the control performance). The resulting two signal components will be transformed to the stationary reference frame, where only the α component (the real voltage component) is used to control the inverter.

2.4. MG Model

In order to validate the proposed WT system within a weak grid, a dynamic MG model was used, were the frequency varies according to the active power balance. The MG voltage is considered not affecting the frequency control mechanism. Therefore, the MG frequency deviation when changing the active power is defined as follows [10]:

$$\Delta f(s) = \frac{-(1 + sT_R) \cdot \Delta P_d(s)}{(Mf_0 T_R) \cdot s^2 + (D \cdot T_R + Mf_0) \cdot s + (D + \lambda_{MG})}, \quad (11)$$

where: Δf - MG frequency deviation following a disturbance; ΔP_d - active power change; T_R - composite time constant of the primary frequency (speed) control of the regulating units within the MG; λ_{MG} - composite power-frequency characteristic of the MG; $M = 2H$ - composite inertial time constant of the MG; D - damping coefficient.

3. Results and Discussion

A 4.5 kW WT was modeled and simulated in Matlab/Simulink and the main results are discussed in the following. Figure 6 shows the steady-state characteristics of the output power and the MPPT effectiveness, defined by (12), when the WT operates in normal conditions, namely no MPP curtailment is applied. It can be observed that the system behaves as expected, extracting maximum power up to the rated wind speed (around 10.5 m/s) and maintaining constant the output power by decreasing the aerodynamic efficiency as the wind speed further increases:

$$MPPT\_EFF[\%] = \frac{P_{WT-meas}}{P_{WT-\max}} \cdot 100, \quad (12)$$

where: $P_{WT\text{-}meas}$, $P_{WT\text{-}\max}$ are the WT measured and maximum available mechanical powers at a given wind speed, as defined by (1).

In order to assess the WT operation under variable MG frequency, a 20 kW MG model, as described in section II-D is implemented. The MG is subjected to an adverse operating scenario, where the generation level exceeds the consumption and the frequency

substantially increases, thus highlighting the proposed power limitation method. A variable wind speed signal, as illustrated in Figure 7, is applied to the wind turbine to mimic a wind gust. Two cases are considered, with and without applying the proposed MPP curtailment. Figure 8 shows the inverter output power and the MG frequency, whereas the variation of the curtailment coefficient k_{md} and the MPPT effectiveness are shown in Figure 9.

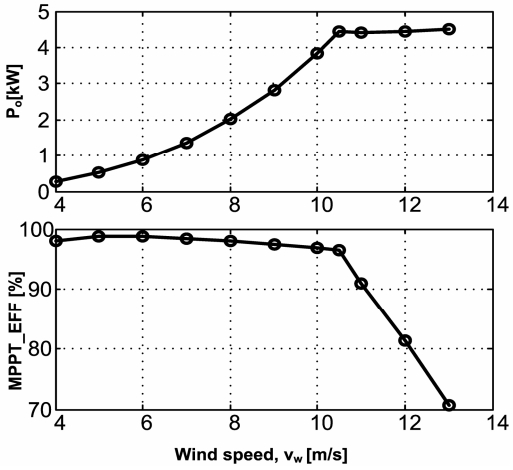

Fig. 6. *Steady-state characteristics:* $P_o = f(v_w)$ *- top;* $MPPT\_EFF = f(v_w)$ *- bottom*

Initially, at t = 1 s a heavy load loss is simulated, which leads to a frequency increase above the 50.5 Hz threshold. After t = 1.5 s, when the wind gust is applied, the MG frequency further increases due to the energy excess. As one can see in Figure 8, without the proposed method the frequency goes up to approximately 50.9 Hz and the WT operates at its optimal operating point. In the second case, with MPP curtailment, the frequency excursion decreases with approximately 0.1 Hz. It can be clearly observed that, during the time the MG frequency surpass the 50.5 Hz threshold, the value of k_{md} decreases below 0.5, while the MPPT effectiveness drops dramatically. The WT output power is reduced by 1 kW, thus supporting the MG frequency.

Regarding the WT rotor operation, Figure 10 shows how the mechanical power and the rotor speed dynamically change during the wind gust. The first curve, from A to B, corresponds to the case when the WT operates at its optimal power regardless the MG frequency, thus no MPP curtailment is applied. In the other case, it can be clearly seen that the new operating points (A_1, B_1) no longer follow the optimal power-speed characteristic because of the curtailment coefficient (k_{md}) action.

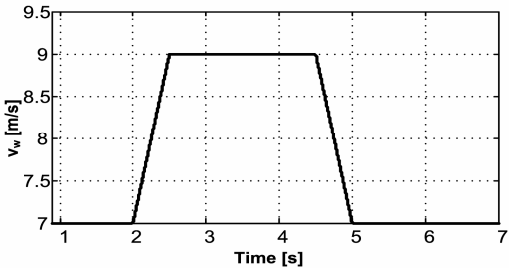

Fig. 7. *Wind speed variation*

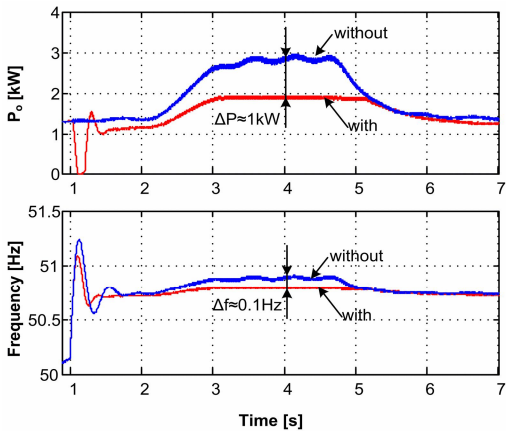

Fig. 8. *Inverter output power and MG frequency, with and without the MPP curtailment technique*

Therefore, as Figure 10 shows, the WT will operate with a certain power reserve (or spinning reserve), depending on the wind speed and MG frequency deviation. By this way, the WT can release the power reserve when the MG requires in a similar way the conventional power plants do.

However, the cost of the energy loss when not harvesting the full wind potential must also be considered. Therefore, it is recommended that the operation in this mode to be shortened as much as possible.

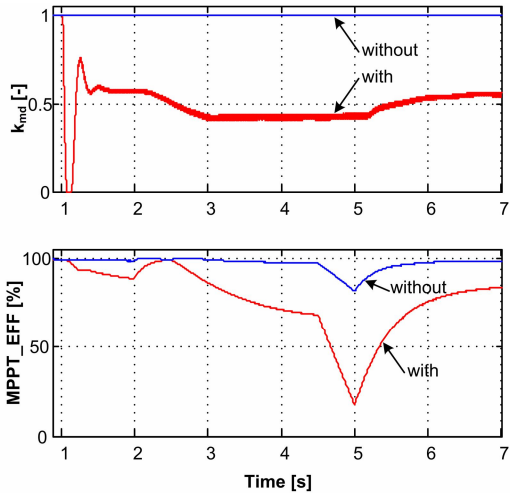

Fig. 9. *MPP curtailment coefficient and MPPT effectiveness, with and without the MPP curtailment technique*

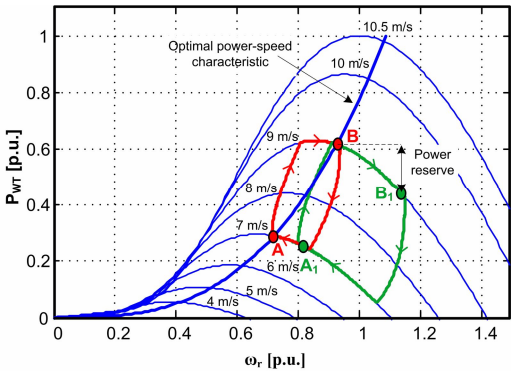

Fig. 10. *WT mechanical characteristics, with loci of operating points, under variable wind speed conditions*

4. Conclusions

This paper presented a sensorless control method for small wind turbines that are integrated in autonomous microgrids. The proposed method enhances the WT control system with a frequency supporting function aiming to reduce the WT output power when the MG frequency exceeds a certain value (50.5 Hz). The maximum power point tracking (MPPT) is ensured by a predefined static characteristic. A curtailment coefficient, which depends on the MG frequency, is used to deflect the WT operating point from the optimal MPP characteristic in order to reduce the aerodynamic efficiency and the WT output power. Simulation results validate the proposed control methods in both steady state and dynamic operating modes. It was proved that the WT could effectively support the MG stability during over-frequency periods.

Future research is intended to be developed towards further improving the transitory regime of the MG frequency by exploiting the inertial response capability of the small WT.

References

1. Bevrani, H., Ghosh, A., Ledwich, G.: *Renewable energy sources and frequency regulation: survey and new perspectives*. In: IET Renewable Power Generation **4** (2010) No. 5, p. 438-457.
2. El Mokadem, M., Courtecuisse, V., Saudemont, C., Robyns, B., Deuse, J.: *Experimental study of variable speed wind generator contribution to primary frequency control.* In: Renewable Energy **34** (2009) No. 3, p. 833-844.
3. Guerrero, J.M., Vasquez, J.C., Matas, J., Vicuna, L.G., Castilla, M.: *Hierarchical Control of Droop-Controlled AC and DC Microgrids - A General Approach toward Standardization.* In: IEEE Trans. Industrial Electronics **58** (2011) No. 1, p. 158-172.
4. Lasseter, R.H.: *Smart Distribution: Coupled Microgrids*. In: Proceedings of the IEEE **99** (2011) No. 6, p. 1074-1082.

5. Mohammad, M., Saeed, G.: *Control strategies for single-phase grid integration of small-scale renewable energy sources: A review*. In: Renewable and sustainable Energy Reviews **16** (2012), p. 4982-4993.
6. Munteanu, I., Bratcu, A.I., Cutululis, N.-A., Ceanga, E.: *Optimal control of wind energy systems e towards a global approach*. Springer-Verlag, USA, 2008.
7. Planas, E., Gil-de-Muro, A., Andreu, A., Kortabarria, I., Martınez de Alegrıa, I.: *General aspects, hierarchical controls and droop methods in microgrids: A review*. In: Renewable & Sustainable Energy Reviews **17** (2013), p. 147-159.
8. Rocabert, J., Luna, A., Blaabjerg, F., Rodriguez, P.: *Control of Power Converters in AC Microgrids*. In: IEEE Trans. Power Electronics **27** (2012) No. 11, p. 4734-4748.
9. Serban, I., Marinescu, C.: *A sensorless control method for variable-speed small wind turbines*. In: Renewable Energy **43** (2012), p. 256-266.
10. Serban, I., Teodorescu, R., Marinescu, C.: *Energy storage systems impact on the short-term frequency stability of distributed autonomous microgrids, an analysis using aggregate models*. In: IET Renewable Power Generation **7** (2013) No. 5, p. 531-539.
11. Siegfried, H.: *Grid Integration of Wind Energy Conversion Systems. Second Edition*. John Wiley & Sons Ltd, USA, 2006.
12. Teninge, A., Jecu, C., Roye, D., Bacha, S., Duval, J., Belhomme, R.: *Contribution to frequency control through wind turbine inertial energy storage*. In: IET Renewable Power Generation **3** (2009), p. 358-370.
13. Teodorescu, R., Lissere, M., Rodriguez, P.: *Grid Converters for Photovoltaic and Wind Power Systems*. Wiley, 2011.
14. Urtasun, A., Sanchis, P., San Martin, I., Lopez, J., Marroyo, L.: *Modeling of small wind turbines based on PMSG with diode bridge for sensorless maximum power tracking*. In: Renewable Energy **55** (2013), p. 138-149.
15. Yingcheng, X., Nengling, T.: *Review of contribution to frequency control through variable speed wind turbine*. In: Renewable Energy **36** (2011) No. 6, p. 1671-1677.